

Application No. 10/762,658
Filed: January 22, 2004
TC Art Unit: 2814
Confirmation No.: 5151

REMARKS

The Examiner's assistance during the interview is gratefully acknowledged and reconsideration of the rejection is respectfully requested in lieu of filing a brief on appeal.

Reconsideration is requested based on the attached publication of Kabasawa et al. (1997). Kabasawa reports that the channel resistance of $Y_{0.9}Pr_{0.1}Ba_2Cu_3O_y/YBa_2Cu_3O_y$ materials increases at thicknesses of 7.5 nm or less. Thus, the basis of the rejection is on the assumption that the materials described by Misewich (see Col. 6, line 47) would operate at the thickness disclosed by Chu. However, this is directly contrary to the results of Kabawasa (see the underlined text at page 2303). Kabawasa state that the "sheet conductance of the channels with thickness less than 5 nm was lower than 10^{-8} s/sq. at room temperature and lower than the resolution limit of the measurement below the critical temperature of YBCO electrodes." Thus, one skilled in the art would not combine the disclosure of Chu with that of Misewich to reject the claims 1-7 and 16-21 under 35 U.S.C. 103(a).

Claims 8-15 and 22-26 have been rejected under 35 U.S.C. 103(a) as being unpatentable over Wei in combination with Song and Ogura.

-6-

WEINGARTEN, SCHURGIN,
GAGNEBIN & LEBOVICI LLP
TEL. (617) 542-2290
FAX. (617) 451-0313

Application No. 10/762,658
Filed: January 22, 2004
TC Art Unit: 2814
Confirmation No.: 5151

Again, Misewich is relied upon for teaching a channel containing a metal, however, the materials of Misewich having insulating characteristics at the thicknesses recited in the claims.

The Examiner is encouraged to telephone the undersigned attorney to discuss any matter that would expedite allowance of the present application.

Respectfully submitted,

DEAN Z. TSANG

By: 

Registration No.
Attorney for Applicant(s)

WEINGARTEN, SCHURGIN,
GAGNEBIN & LEOVICI LLP
Ten Post Office Square
Boston, MA 02109
Telephone: (617) 542-2290
Telecopier: (617) 451-0313

TOH/trb/361772.1

Electric field effect on the transport properties of ultrathin $Y_{0.9}Pr_{0.1}Ba_2Cu_3O_y$ channels in the insulating phase of superconductor-insulator transition

U. Kabasawa,^{a)} H. Hasegawa,^{b)} T. Fukazawa,^{b)} Y. Tarutani,^{b)} and K. Takagi^{b)}
Central Research Laboratory, Hitachi, Ltd., 1-280, Higashi-Kogakubo, Kokubunji, Tokyo 185, Japan

(Received 12 August 1996; accepted for publication 4 November 1996)

The electric field effect on the transport properties of ultrathin $Y_{0.9}Pr_{0.1}Ba_2Cu_3O_y$ channels was examined as a function of channel thickness and channel length. Samples having a planar $YBa_2Cu_3O_y$ ultrathin $Y_{0.9}Pr_{0.1}Ba_2Cu_3O_y$ - $YBa_2Cu_3O_y$ structure with a gate electrode on the backside of their $SrTiO_3$ substrate were used. The channel layer exhibited superconducting properties when its thickness was more than 9 nm, whereas channels less than 7.5 nm thick were in the insulating phase of the superconductor-insulator transition. The modulation ratio of the conductance of the insulating (I)-phase channels was a few orders of magnitude higher than the modulation ratio of the carrier density. The field-effect mobility increased with increasing channel thickness when the film was in the insulating phase. The sheet conductance of channels shorter than 10 μm was higher than that of a 100- μm -long channel of the same thickness due to a size effect on the transport of the I-phase $Y_{0.9}Pr_{0.1}Ba_2Cu_3O_y$ channel. The field-effect mobility was also enhanced by the size effect. These results imply that the performance of possible field-effect transistors with high-temperature superconductors may be much improved by utilizing an I-phase channel whose length is short enough for the size effect to be evident. © 1997 American Institute of Physics. [S0021-8979(97)00904-3]

I. INTRODUCTION

Investigation of the ways in which the transport characteristics of high-temperature superconductors (HTSCs) are affected by electric field has demonstrated the potential utility of these materials as the channel layers of field-effect devices.¹⁻⁵ The current modulation by the electric field effect has been successfully demonstrated. However, the current modulation ratio at low temperatures has generally been much smaller than unity even when the thin film used as a gate insulator was made of a material with a high dielectric constant, such as $SrTiO_3$ or $(Ba,Sr)TiO_3$. This is probably because the current modulation ratio is limited to the level of the carrier density modulation ratio. Since the carrier density in HTSCs is more than three orders of magnitude higher than that in doped semiconductors, the ratio of carrier density modulation due to the electric field effect is inevitably much lower than unity, even when the HTSC channel layer is only a few unit cells thick.

It was recently shown that ultrathin $Y_{0.9}Pr_{0.1}Ba_2Cu_3O_y$ ($Y_{0.9}Pr_{0.1}BCO$) films undergo a superconductor-insulator (S-I) transition when film thickness is reduced sufficiently.⁶ These films exhibited insulating properties when the normal sheet conductance of the film was reduced to less than the quantum sheet conductance, $4e^2/h$. Furthermore, the ratio of conductance modulation due to the electric field effect was much larger for insulating (I)-phase ultrathin $Y_{0.9}Pr_{0.1}BCO$ films than for superconducting (S)-phase films.⁶ This indicates that in the I phase there may be a novel electric field

effect mechanism enabling the efficient modulation of transport properties. The transport properties of I-phase films are thought to be quite different from those of the semiconductors usually used for field-effect transistors (FETs), and systematic study is needed in order to clarify both the behavior of carrier transport in I-phase films and the ways in which this transport is affected by electric field.

In this article we report the transport properties of ultrathin $Y_{0.9}Pr_{0.1}BCO$ channels in the insulating phase and the electric field effect on these properties for various channel thicknesses and channel lengths. The temperature dependence of channel conductance, the current-voltage characteristics of I-phase channels, and the conductance modulation caused by the electric field were systematically examined. The field-effect mobility in I-phase channels was also evaluated to determine the feasibility of field-effect devices with an I-phase channel.

II. EXPERIMENT

We fabricated samples having a planar $YBa_2Cu_3O_y$ ultrathin $Y_{0.9}Pr_{0.1}BCO$ - $YBCO$ structure with a gate electrode on the backside of their $SrTiO_3$ substrate. The structure of the samples is shown in cross section in the inset of Fig. 2(A). A 30-nm-thick $YBCO$ layer was first deposited on a 0.7- μm -thick $SrTiO_3$ (100) substrate by pulsed laser deposition in an oxygen atmosphere of 0.2 Torr. The KrF excimer laser with a wavelength of 248 nm was used, and substrate temperature was kept at 720 °C during the deposition. After the electrode pattern of this layer was formed by electron beam lithography and in beam etching using argon, a $Y_{0.9}Pr_{0.1}BCO$ layer was deposited in the area between the $YBCO$ electrodes. The substrate temperature and oxygen pressure for this deposition were the same as those for the $YBCO$ deposition. The power density of the laser pulse was

^{a)}Present address: Electronic Device Manufacturing Equipment and Engineering Division, Hitachi, Ltd., 6 Kanda-Surugadai 4-chome, Chiyoda-ku, Tokyo 100, Japan.

^{b)}Present address: Advanced Research Laboratory, Hitachi, Ltd., Hitachinaka, Saitama 350-03, Japan.

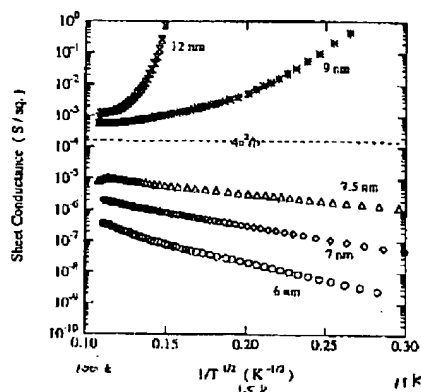


FIG. 1. Temperature dependence of sheet conductances for ultrathin $Y_{0.9}Pr_{0.1}BCO$ channels of various thicknesses. Channel length and width were 100 and 800 μm .

2.3 J/cm^2 . The deposition rate was 0.03 nm/shot, and the channel thickness was controlled by the total repetition number of the laser pulse shots which were irradiated on the oxide target at 1 Hz. Finally, the Au gate electrode was deposited on the back of the substrate.

The temperature dependence of the conductance between the YBCO electrodes was measured from 10 K to the superconducting critical temperature of the YBCO electrodes. The current-voltage characteristics between the electrodes were measured at gate voltages below 100 V.

III. RESULTS AND DISCUSSIONS

A. Thickness dependence

We measured the transport properties of ultrathin $Y_{0.9}Pr_{0.1}BCO$ films and evaluated the electric field effect as a function of thickness by using samples having channels with a length (L) of 100 μm and a width (W) of 800 μm . The temperature (T) dependence of the sheet conductance (G_s) of the channels is shown on a $\log G_s - 1/T^{1/2}$ scale in Fig. 1. The superconducting critical temperature of YBCO electrodes in these samples was about 80 K ($\sim 0.11 K^{-1/2}$). The G_s value is defined as $G \times (L/W)$, where G is the channel conductance. Superconducting properties were observed for the channels with a film thickness above 9 nm. At thicknesses of 7.5 nm or less, insulating properties were observed. The sheet conductance of the channels with thickness less than 5 nm was lower than $10^{-6} S/sq.$ at room temperature, and lower than the resolution limit of the measurement below the critical temperature of YBCO electrodes. The sheet conductances of the insulating films were lower than the quantum sheet conductance, $4e^2/h$. If we assume that the critical sheet conductance for the S-I transition is exactly $4e^2/h$ (0.155 mS), we can estimate the critical thickness to be ~ 8.5 nm. The temperature dependence of the conductance for I-phase films can be expressed approximately as $G_s = G_{\infty} \exp\{-(T_0/T)^x\}$, with exponent x below 0.5 at low

J. Appl. Phys., Vol. 81, No. 5, 1 March 1997

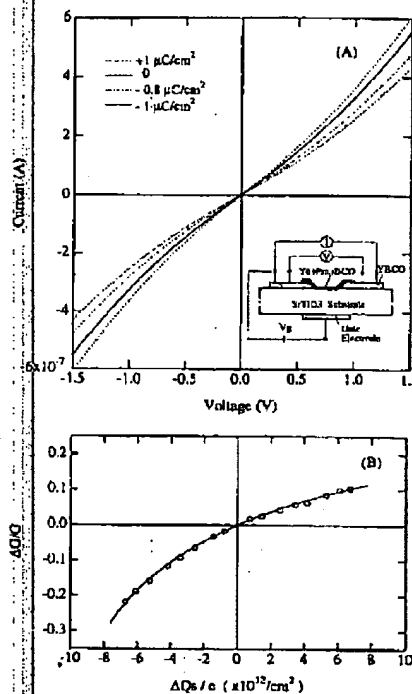


FIG. 2. Current-voltage curves with and without charge modulation (A) and conductance modulation ratio as a function of the charge modulation (B) for an insulating phase $Y_{0.9}Pr_{0.1}BCO$ channel at 10 K. Channel length, width, and thickness were 100 μm , 800 μm , and 7 nm.

temperatures. This temperature dependence is more like that of variable-range-hopping (VRH) transport in a localized carrier system than it is like that of the transport in ordinary insulators with a finite energy gap for the mobile-carrier excitation.

An example of the current-voltage ($I-V$) characteristics in an I-phase $Y_{0.9}Pr_{0.1}BCO$ channel and the effect of modulation caused by the electric field are shown in Fig. 2(A). The thickness of this channel was 7 nm. The solid line shows the $I-V$ curve obtained when no gate voltage was applied. Nonlinearity in the $I-V$ curve is characteristic of localized carrier systems.^{7,8} The current clearly changed with charge density modulation. The amount of charge density modulation (ΔQ_s) in the $Y_{0.9}Pr_{0.1}BCO$ channel was calculated from the applied gate voltage and the dielectric constant of $SrTiO_3$ substrate, which depended on the applied electric field.⁹ The charge density was modulated by $-1 \mu C/cm^2$ at a gate voltage of +100 V. Although this amount of charge modulation was more than one order of magnitude smaller than that obtained when using a thin-film gate insulation,² the modulation ratio of the current was as high as 22%. The sheet carrier density (N_s) of a 7-nm-thick channel

Kabasawa et al. 2303

was estimated to be $3.5 \times 10^{15} \text{ cm}^{-2}$, and the carrier density modulation ratio $\Delta N_s/N_s$ in the channel under the charge modulation of $1 \mu\text{C}/\text{cm}^2$ was estimated to be 0.18%. The current (or conductance) modulation ratio for the 7-nm-thick channel was thus about 120 times higher than the carrier density modulation ratio. In conventional field-effect devices, the modulation ratio of the channel conductance is about the same as the modulation ratio of the carrier density because conductivity is proportional to carrier density in itinerant-carrier systems. For 1-phase $\text{Y}_{0.9}\text{Pr}_{0.1}\text{BCO}$, the results of the electric field effect are obviously different for those for an itinerant-carrier system.

The conductance modulation ratio ($\Delta G/G$) is shown as a function of the charge modulation in Fig. 2(B). Channel conductance G is defined as I/V , and ΔG is the deviation of G caused by charge modulation. The $\Delta G/G$ value was almost invariable for bias voltage. The relation of $\Delta G/G$ to ΔQ has nonlinear asymmetrical properties. This means the ratio of conductance modulation to carrier density modulation, $(\Delta G/G)/(\Delta N_s/N_s)$, is not constant. It becomes much larger when ΔN_s takes a larger absolute value in the negative direction.

The carrier transport in 1-phase films is estimated to be similar to that in Efros-Shklovskii-type VRH system.^{10,31} Localization length ξ (decay length of localized wave function) is the parameter determining the transport properties. Conductance G is written as

$$G = G_0 \exp[-(Cq^2/\epsilon\xi k_B T)^{1/2}], \quad (1)$$

where q is the carrier charge and ϵ is the dielectric constant. If $\xi + \Delta\xi$ is substituted for ξ in Eq. (1), G becomes a nonlinear function of $\Delta\xi$, with stronger dependency for negative $\Delta\xi$ than for positive $\Delta\xi$. In an experiment on the thickness-dependent S-I transition,¹² the effective disorder level for the carrier system in the film was assumed to be increased by reducing the thickness. Similarly, carrier density modulation may also change the effective disorder level. Since the carriers in $\text{Y}_{0.9}\text{Pr}_{0.1}\text{BCO}$ have positive charge, the positive (negative) charge modulation is assumed to change the localization length by a positive (negative) value, through changing the relative disorder level for the carrier system. The solid line in Fig. 2(B) is an example of the $\Delta G/G - \Delta Q$ curve calculated using Eq. (1) under the assumption that $\Delta\xi$ is simply proportional to ΔQ , (or ΔN_s). Nonlinearity similar to that for the observed conductance modulation is well expressed under this simple assumption. Though detailed studies on the relation between ΔN_s and $\Delta\xi$ are needed to clarify the quantitative aspects of this nonlinear modulation property, it seems valid to assume that the conductance modulation is principally caused by modulation of the localization parameter.

We next compare conductance modulation between channels with different thicknesses. The relation between sheet conductance G_s and conductance modulation $|\Delta G_s|$ under a charge modulation ΔQ , of $-1 \mu\text{C}/\text{cm}^2$ at 10 K is shown in Fig. 3. The channel thicknesses d ranged from 6 nm (for $G_s = 10^{-9} \text{ S}$) to 7.5 nm (for $G_s = 10^{-6} \text{ S}$). Although $|\Delta G_s|$ was not strictly constant when the bias voltage changed because of the nonlinearity in the $I-V$ characteris-

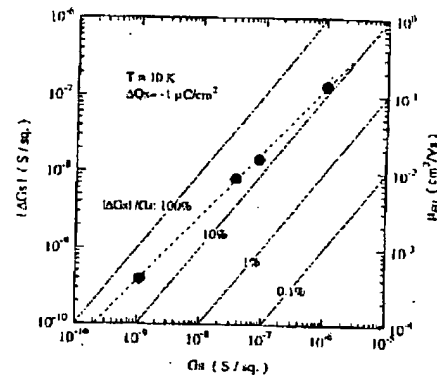


FIG. 3. Sheet conductance modulation ΔG_s (under $-1 \mu\text{C}/\text{cm}^2$ charge modulation) as a function of sheet conductance G_s . Solid lines are contours of the constant conductance modulation ratio. The right-hand axis scale is the field-effect mobility defined as $\Delta G_s/\Delta Q$.

tics, the dependency was weak for the measured bias voltage, which was typically below 1 V (or the bias field being below 100 V/cm). The ΔG_s increased with increasing G_s , or increasing channel thickness d . For itinerant-carrier systems, such as those in conventional metals or well-crystalline semiconductors, $\Delta G_s/\Delta Q$ equals drift mobility μ , which is essentially constant for the same material. The observed ΔG_s , however, varied by orders of magnitude under a constant ΔQ , when the thickness was changed.

The solid lines in Fig. 3 are the contours for conductance modulation ratio $|\Delta G_s|/G_s$, and the data points measured for four samples are all above the 10% line. Under a charge modulation of $1 \mu\text{C}/\text{cm}^2$, the ratio of the carrier density modulation $|\Delta N_s|/N_s$ for these samples was 0.15%–0.2%. The values of $|\Delta G_s|/G_s$ for these samples were thus more than two orders of magnitude larger than $|\Delta N_s|/N_s$. Extrapolating these points to the critical sheet conductance value of $4e^2/h$, we estimate the conductance modulation ratio to be about 6% at the S-I transition point. This is still more than an order of magnitude larger than the carrier density modulation ratio. In contrast, the conductance modulation ratio was far less than 0.1% for the channels on the superconducting side of the S-I transition: the value of $|\Delta G_s|/G_s$ was less than that of $|\Delta N_s|/N_s$. A field effect with a ratio $(\Delta G_s/G_s)/(\Delta N_s/N_s)$ being much larger than unity was found to be characteristic only for the insulating side of the S-I transition.

Though the drift mobility cannot be simply defined for 1-phase $\text{Y}_{0.9}\text{Pr}_{0.1}\text{BCO}$, evaluation of the apparent field-effect mobility, defined as $\mu_{\text{FET}} = \Delta G_s/\Delta Q$, is still important because this mobility is proportional to the transconductance of FETs, which is related to possible device-performance parameters such as voltage gain and cutoff frequency. If the definition of μ_{FET} is formally applied to 1-phase $\text{Y}_{0.9}\text{Pr}_{0.1}\text{BCO}$, μ_{FET} is a function of channel thickness d .

Kabasawa et al.

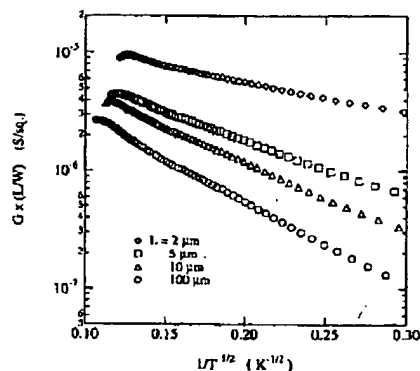


FIG. 4. Temperature dependence of channel sheet conductance for 7.2-nm-thick channels of various length L . Channel widths were 800 μm for $L=100$ μm , 200 μm for $L=10$ μm , and 100 μm for $L=2$ and 5 μm .

charge density modulation ΔQ_s , and in-plane electric field E . The dependency on E is weak within the measured bias range, so it is neglected here. The μ_{FE} at $\Delta Q_s = -1$ $\mu\text{C}/\text{cm}^2$ was directly evaluated from the ΔG_s data in Fig. 3, as shown on the right-hand axis. The field-effect mobility of I -phase films increased from 3×10^{-4} to $0.13 \text{ cm}^2/\text{V s}$ with increasing thickness from 6 to 7.5 nm. The μ_{FE} at the S-I transition point—the maximum possible μ_{FE} for I -phase $\text{Y}_{0.9}\text{Pr}_{0.1}\text{BCO}$ —was estimated by extrapolation to be about 9 $\text{cm}^2/\text{V s}$. This is much higher than the field-effect mobility observed on nonsuperconducting YBCO and La_2CuO_4 at low temperatures^{13,14} and is comparable to the field-effect mobility of superconducting YBCO immediately above the critical temperature.¹³

Although a high conductance modulation ratio $\Delta G/G$ was obtained for I -phase channels, the field-effect mobility was still smaller than the mobility in semiconductors (10^3 – 10^5 $\text{cm}^2/\text{V s}$) (as far as channels with a length scale of 100 μm were used). The field-effect mobility is proportional to the deviation of sheet conductance, ΔG_s , which is inherently small for I -phase film because the sheet conductance G_s is less than $4e^2/h$. For I -phase film to be made practical for use in FETs, a way to obtain higher conductance must be developed.

B. Channel-length dependence

To evaluate the sheet conductance of the channels as a function of channel length, we simultaneously formed a set of channels with the same thickness on a single substrate. The temperature dependence of the conductance of these channels is shown in Fig. 4. The channels were 7.2 nm thick, their lengths ranged from 2 to 100 μm , and the channels were wider than they were long. The ordinate axis shows the sheet conductance of the channel layer. The sheet conductances became higher for shorter channels when the channel length was less than 10 μm . This is a size effect that changes the in-plane transport properties of the I -phase $\text{Y}_{0.9}\text{Pr}_{0.1}\text{BCO}$

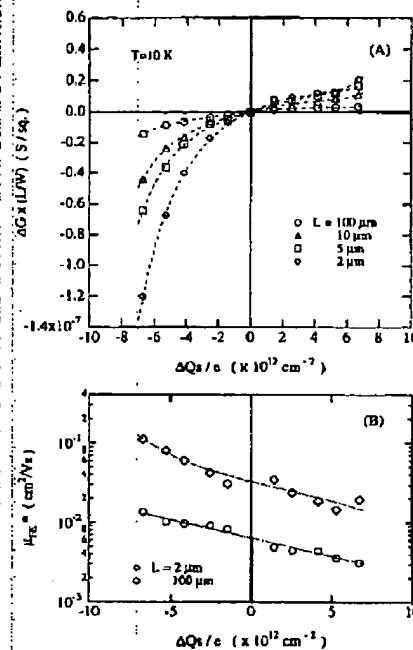


FIG. 5. Modulation of sheet conductance $\Delta G \times (L/W)$ as a function of charge modulation for channels with lengths of 2–100 μm (A). Field-effect mobility as a function of charge density modulation for 2- and 100- μm -long channels (B). Channel thickness was 7.2 nm.

film. The sheet conductance of a channel is increased by the size effect when the channel length is of the order of micrometers.

The enhancement of conductance by the size effect has been observed for the VRH transport of disordered systems, such as amorphous semiconductors, when the electrode distance is small enough to be comparable to the hopping distance of carriers.¹⁶ However, the typical length scale of the size effect in such systems is only of the order of 10 nm. The length scale of the observed size effect is extremely long, implying that the localization of carriers is much weaker for these systems than it is for conventional VRH systems.

The sheet conductance of these channels was measured at 10 K with and without an applied electric field. The relation between sheet conductance modulation and charge modulations is shown in Fig. 5(a). Nonlinear behavior of conductance modulation similar to the modulation shown in Fig. 2(b) was observed for all channels. This indicates that the electric field-effect mechanism, which causes conductance modulation in long channels, still plays a role even when the channel conductance is enhanced by the size effect. Modulation of the localization parameter may also cause conductance modulation in short channels. The amount of sheet conductance deviation $\Delta G \times (L/W)$ was higher for

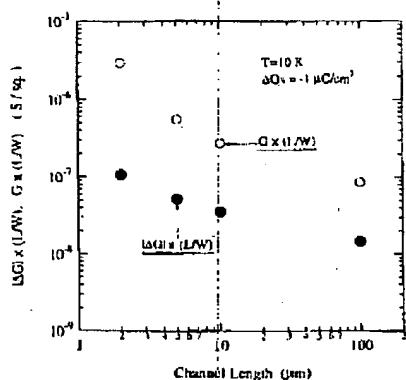


FIG. 6. Sheet conductance $G \times (L/W)$ and its modulation $\Delta G \times (L/W)$ due to a charge modulation of $-1 \mu\text{C}/\text{cm}^2$ as a function of channel length. Channel thickness was 7.2 nm.

shorter junctions. The nonlinearity of sheet conductance modulation means that field-effect mobility μ_{FE} for finite-sized channels depends on charge density modulation ΔQ_s , if nominal field-effect mobility in finite-sized channels is defined as $\mu_{FE} = \Delta K \times (L/W) / \Delta Q_s$. The field-effect mobility of 2- and 100- μm -long channels is shown as a function of charge density modulation in Fig. 5(B). It was much higher for a negative ΔQ_s with a larger absolute value.

Sheet conductance $G \times (L/W)$ and its modulation $|\Delta G \times (L/W)|$ under a charge modulation of $-1 \mu\text{C}/\text{cm}^2$ are plotted as a function of channel length in Fig. 6. The amount of the conductance modulation also increased with decreasing channel length, with the size-effect-induced enhancement of sheet conductance. Although the increase in the modulation $\Delta G \times (L/W)$ is not the same as that in $G \times (L/W)$, the larger amount of modulation for shorter channels indicates that nominal field-effect mobility is enhanced by the size effect. The field-effect mobility for these finite-sized channels was increased from 0.014 to 0.1 cm^2/Vs by shortening the channel length from 100 to 2 μm .

To summarize the influence of the field effect on finite-sized I-phase channels, the nominal field-effect mobility can be represented by function $\mu_{FE}(L, d, \Delta Q_s, E)$, where L and d are channel length and thickness, ΔQ_s is charge density modulation, and E is the in-plane electric field. The complexity of this function arises from the fact that carrier localization in I-phase $\text{Y}_{0.9}\text{Pr}_{0.1}\text{BCO}$ makes the field-effect mechanism quite different from that in semiconductors. The modulation of the localization parameter caused by carrier density modulation, rather than the carrier density modulation itself, is supposed to play an essential role on the modulation of the transport properties. The field-effect mobility is remarkably increased by decreasing length L , by increasing thickness d within I-phase side, or by increasing charge density modulation $|\Delta Q_s|$ in the negative direction. Although the maximum field-effect mobility actually observed in this study was as low as $\sim 0.1 \text{ cm}^2/\text{Vs}$, the field-effect mobility

can be increased by several orders of magnitude by selecting appropriate values for parameters L and d simultaneously; setting L below a micrometer and d as close as possible to the critical thickness of the S-I within the I-phase side. Increasing the charge density $|\Delta Q_s|$ by using a thin-film gate insulator will also enhance the field-effect mobility exponentially.

Furthermore, the fact that both the sheet conductance and the field-effect mobility can be enhanced by decreasing the channel length indicates the possibility of a new principle for superconducting field-effect devices. The supercurrent is finally observed through a localized carrier system (a VRH system such as $\alpha\text{-Si}$) when the distance between the superconducting electrodes is sufficiently decreased.^{17,18} Recently, the transport properties of all-oxide superconducting junctions with a semi-insulating barrier, such as $\text{PrBa}_2\text{Cu}_3\text{O}_x$, have also been discussed in relation to the size effect on VRH systems.¹⁹ Note only quasi particles, but also superconducting carriers may be transported via localized states.²⁰ The size effect on the transport in I-phase $\text{Y}_{0.9}\text{Pr}_{0.1}\text{BCO}$ indicates the possibility that the I-phase channels also exhibit superconducting properties when the distance between superconducting electrodes is small enough.

The localization parameter in the VRH system has usually been regarded as a fixed parameter for the material, so junctions with a barrier material containing a localized carrier system have been investigated as mere two-terminal elements. The I-phase $\text{Y}_{0.9}\text{Pr}_{0.1}\text{BCO}$ may be the first system in which both the size effect and the considerably large electric field effect on transport properties have been observed, indicating that the localization parameters can be controlled by applying electric field. The superconducting current density is expected to be exponentially dependent on the localization parameter when the superconducting carriers are transported via the localized carrier system.²⁰ The supercurrent may thus be sensitively controlled by the electric field through the modulation of the localization parameter, by using the I-phase channel as a coupling layer of the superconducting planar junction. This must result in remarkable improvement in the nominal field-effect mobility for the channel because a much larger amount of conductance modulation is expected when the supercurrent (or infinitely large conductance) can be controlled. Quantitative relations such as the carrier concentration dependence of the localization parameter and the dependence of possible superconducting current on the localization parameter, however, are not yet clearly understood. Learning more about these relations will provide a better perspective on possible superconducting field-effect devices utilizing I-phase channels.

IV. SUMMARY

The transport properties of ultrathin $\text{Y}_{0.9}\text{Pr}_{0.1}\text{BCO}$ channels, and the electric field effect on these properties were systematically examined in order to evaluate the ways in which they are influenced by channel thickness and channel length. Samples having a planar YBCO ultrathin $\text{Y}_{0.9}\text{Pr}_{0.1}\text{BCO}$ -YBCO structure with a gate electrode on the backside of their SrTiO_3 (100) substrate were used. Channel layers with thickness less than 7.5 nm were in the insulating

phase of the S-I transition, while superconducting properties were observed at thicknesses greater than 9 nm. In the I-phase, the modulation ratio of the channel conductance was a few orders of magnitude higher than the carrier density modulation. Below the critical thickness of the S-I transition, the field-effect mobility increased with increasing layer thickness. The sheet conductances of channels shorter than 10 μm were higher than those of long channels due to the size effect. The field-effect mobility was also enhanced by the size effect.

ACKNOWLEDGMENTS

This work was carried out by the Superconducting Electron Devices Project under the management of the R&D Association for Future Electron Devices (FED) as a part of the Ministry of International Trade and Industry (MITI) R&D of Industrial Science and Technology Frontier Program supported by New Energy and Industrial Technology Development Organization (NEIDO). The authors thank Dr. M. Miyao for his encouragement throughout this work.

- ¹J. Mannhart, D. G. Schlom, J. G. Bednorz, and K. A. Müller, *Phys. Rev. Lett.* **67**, 2099 (1991).
- ²T. Frey, J. Mannhart, J. G. Bednorz, and R. J. Williams, *Phys. Rev. B* **51**, 3257 (1995).

- ³X. Xi, Q. Li, C. Doughty, C. Kwon, S. Bhattacharya, A. T. Furdikoglou, and T. Venkatesan, *Appl. Phys. Lett.* **59**, 3470 (1991).
- ⁴K. Matsui, T. Awaaji, T. Hirano, T. Fujii, K. Sukata, and T. Kobayashi, *Jpn. J. Appl. Phys.* **31**, 1342 (1992).
- ⁵R. Schneider and R. Auer, *Appl. Phys. Lett.* **67**, 2075 (1995).
- ⁶U. Kabasawa, Y. Torutani, T. Fukazawa, N. Sugii, H. Hasegawa, and K. Takagi, *J. Appl. Phys.* **79**, 7849 (1996).
- ⁷U. Kabasawa, Y. Torutani, A. Tsukamoto, T. Fukazawa, M. Hirasani, and K. Takagi, *Physica C* **194**, 261 (1992).
- ⁸A. Apsley and H. P. Hughes, *Philos. Mag.* **31**, 1327 (1975).
- ⁹C. Neville, B. Hoeneisen, and C. A. Mead, *J. Appl. Phys.* **43**, 2129 (1975).
- ¹⁰M. P. A. Fisher, *Phys. Rev. Lett.* **65**, 923 (1980).
- ¹¹A. L. Efros and B. I. Shklovskii, *J. Phys. C* **8**, L49 (1975).
- ¹²Y. Liu, D. B. Haviland, B. Neuse, and A. M. Goldman, *Phys. Rev. B* **47**, 5831 (1993).
- ¹³A. Levy, J. P. Fulek, M. A. Kastner, R. J. Birgeneau, and A. T. Fiory, *Phys. Rev. B* **51**, 648 (1995).
- ¹⁴A. Levy, J. P. Fulek, M. A. Kastner, R. J. Birgeneau, A. T. Fiory, A. E. Hsian, W. J. Gallagher, A. W. Kleinwasser, and A. C. Anderson, *Phys. Rev. B* **46**, 520 (1992).
- ¹⁵A. T. Fiory, A. E. Hsian, R. H. Eick, P. M. Mankiewicz, R. E. Howard, and M. L. O'Malley, *Phys. Rev. Lett.* **65**, 3441 (1990).
- ¹⁶Y. Xu, A. Matsuura, and M. R. Heasley, *Phys. Rev. B* **42**, 1492 (1990).
- ¹⁷J. Halbritter, *Surf. Sci.* **122**, 80 (1982).
- ¹⁸P. Bradley, W. Ruby, D. Heber, and T. Van Duzer, *J. Appl. Phys.* **66**, 4872 (1989).
- ¹⁹U. Kabasawa, Y. Torutani, M. Okamoto, T. Fukazawa, A. Tsukamoto, M. Hirasani, and K. Takagi, *Phys. Rev. Lett.* **70**, 1700 (1993).
- ²⁰I. A. Devyatov and A. L. Yu. Kupelyanov, *Pis'ma Zh. Eksp. Teor. Fiz.* **59**, 187 (1994); *JETP Lett.* **59**, 200 (1994).